

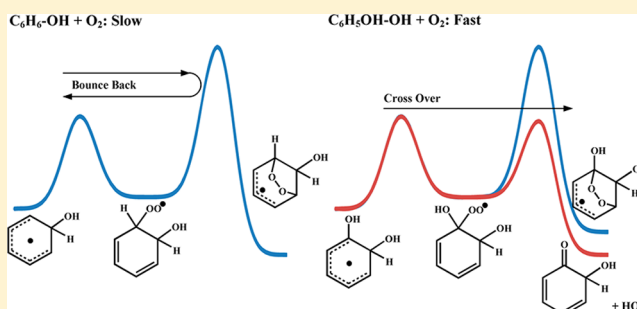
Atmospheric Oxidation Mechanism of Phenol Initiated by OH Radical

Cui Xu and Liming Wang*

School of Chemistry & Chemical Engineering and The Key Laboratory of Fuel Cell Technology of Guangdong Province, South China University of Technology, Guangzhou, 510640, China

Supporting Information

ABSTRACT: The gas-phase oxidation mechanism of phenol initiated by OH radical was investigated using DFT and ab initio calculations. The initiation of the reaction is dominated by OH addition to *ortho*-position, forming P2, which subsequently combines with O₂ at the *ipso*-position to form P2-1-OO adduct. A concerted HO₂ elimination process from P2-1-OO was found to be much faster than the common ring closure to bicyclic intermediates. The HO₂ elimination process from P2-1-OO forms 2-hydroxy-3,5-cyclohexadienone (HCH) as the main product and is also responsible for the experimental fact that the rate constants for reaction between P2 and O₂ are about 2 orders of magnitude higher than those between other aromatic–OH adducts and O₂. It was speculated that HCH would isomerize to catechol, which is thermodynamically more stable than HCH and was the experimentally observed main product, possibly through heterogeneous processes. Reaction of P2 with NO₂ proceeded by addition to form P2-*n*-NO₂ (*n* = 1, 3, 5), followed by HONO elimination from P2-1/3-NO₂ to form catechol. The barriers for HONO elimination and catechol formation are below the separate reactants P2 and NO₂, being consistent with the experimental observation of catechol in the absence of O₂, while H₂O elimination from P2-1/3-NO₂ to form 2-nitrophenol (2NP) is hindered by high barriers. The most likely pathway for 2NP is the reaction of phenoxyl radical and NO₂.



1. INTRODUCTION

Phenol and alkyl-substituted phenols are of concern because of their potential harm to human health and wildlife. The sources for atmospheric phenol are mainly of anthropogenic origin, including the production and uses of phenol itself and its products, such as phenolic resins and caprolactam, vehicle exhaust, residential wood burning, cigarette smoke, and so forth. Atmospheric phenol was also formed with high yields from the reaction of benzene and OH radical at low NO_x conditions^{1–3} and alkyl-substituted phenols from reactions of substituted benzenes;^{3–5} consequently, the phenolic compounds and their oxidation products in both gaseous and aqueous phases may contribute significantly to secondary organic aerosol formation in the atmospheric oxidation of aromatic compounds.^{5–7}

The gas-phase oxidation of phenol in the atmosphere is initiated by its reactions with OH radical during the daylight hours and with NO₃ during the nighttime. The rate constants have been measured for reactions of phenol^{8–10} and substituted phenols^{10–13} with OH and NO₃. In the presence of tens of ppm of NO_x, products observed in the gas-phase reaction of phenol and OH have been identified as catechol (1,2-dihydroxybenzene), *o*-nitrophenol, and *p*-benzoquinone with the yield of 70–80% for catechol and only a few percent for the others as measured by in situ FTIR absorption spectroscopy,^{6,10,14} while the oxidation of phenol by OH in the aqueous phase produced catechol and *p*-benzoquinone with yields of ~45% and ~30%.¹⁵ The reaction of phenol and the OH radical can proceed via OH

additions to the aromatic ring or phenolic H-abstraction. It has been suggested that the additions lead to the formation of catechol, while the H-abstraction to nitrophenol and benzoquinone. However, the mechanism has not received much confirmation. In this paper, we present a detailed theoretical investigation on the atmospheric oxidation mechanism of phenol based on quantum chemistry and transition state calculations.

2. COMPUTATIONAL METHODS

The geometries were optimized and vibrational frequencies were calculated using density functional method BH&HLYP with 6-311++G(2df,2p) basis set. Transition states were verified by one imaginary vibrational frequency, by viewing the displacement vector, and for ambiguous ones by intrinsic reaction coordinate (IRC) calculations. Because of the heavy spin contamination which is typical for delocalized aromatic rings and for O₂ additions, the electronic energies were further calculated at CCSD(T)/6-311+G(d,p) level with restricted open-shell wave function (ROCCSD(T)).¹⁶ The reaction rate constants were estimated using the traditional transition state theory with the BH&HLYP zero-point energies, vibrational frequencies, and geometries and the ROCCSD(T) electronic energies. All the

Received: September 6, 2012

Revised: February 22, 2013

Published: February 26, 2013

density functional theory (DFT) and molecular orbital calculations were performed using Gaussian 09 package.¹⁷

3. RESULTS AND DISCUSSION

3.1. Initial Addition and Phenolic H-Abstractions. The initial step of the reaction is the formation of prereactive complexes between phenols and OH. Three distinguishable complexes, *PRC1*–*PRC3*, were identified, of which *PRC1* and *PRC2* have hydrogen bonds and *PRC3* has the OH radical sitting almost normal to the aromatic ring with the H-atom pointing to the benzene ring (Figure 1). Obviously, *PRC1* serves as

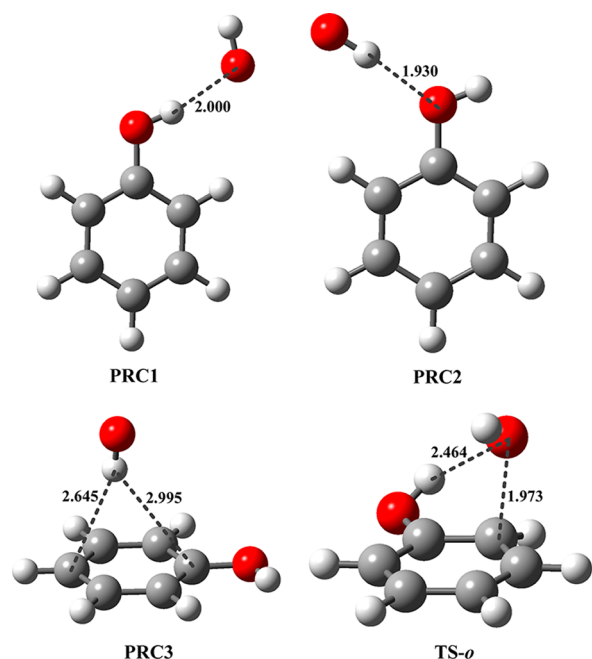


Figure 1. BH&HLYP/6-311++G(2df,2p) geometries for the pre-reaction complexes (*PRC*) and transition state of *o*-addition between phenol and OH radical (bond lengths in Å).

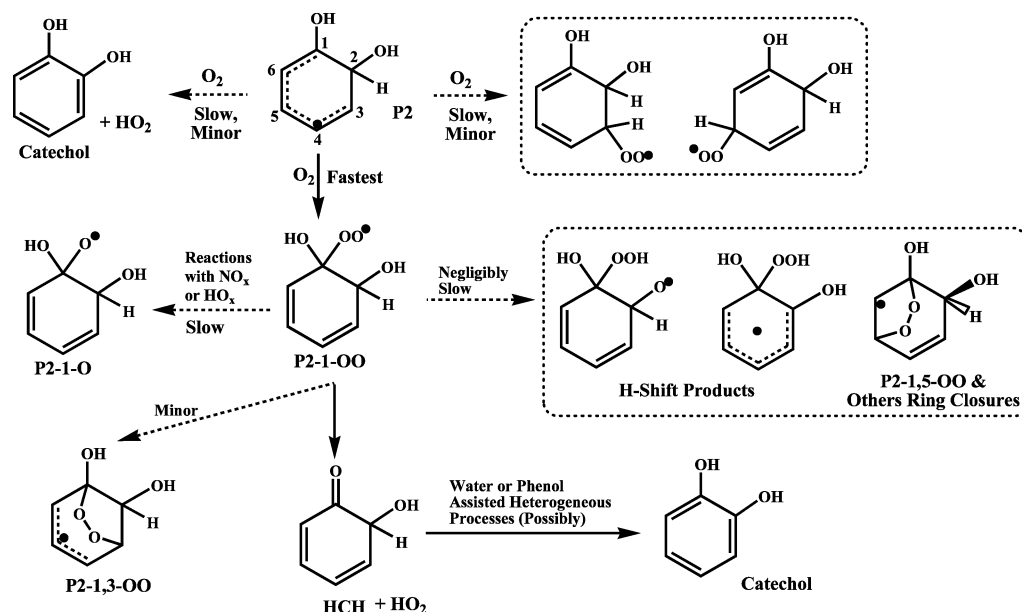
intermediate for the phenolic H-abstraction and *PRC3* for OH additions to the aromatic ring by flipping the OH moiety. At ROCCSD(T) level, *PRC1*–*PRC3* are found to be stabilized by 16.7, 17.5, and 15.6 kJ/mol, respectively.

According to the experimental results by Knispel et al.,⁸ the reaction of phenol and OH radical is dominated by OH addition with negligible branching for the phenolic H-abstraction under the atmospheric conditions. Six transition states were identified here at BH&HLYP level for OH additions, discriminating the differences between two *ortho*-additions (*o*- and *o'*-) and two *meta*-additions (*m*- and *m'*-). The barrier heights at ROCCSD(T) level are 0.2, −8.6 and 2.6, 8.0 and 10.5, and 3.5 kJ/mol for *ipso*-, two *ortho*-, two *meta*-, and *p*-additions, respectively, relative to the separated phenol and OH. The barrier for one of the *ortho*-additions (TS-*o* in Figure 1) is the lowest because of the intramolecular hydrogen bond formed between incoming OH and the phenolic hydrogen atom.

A simple estimation using the traditional transition state theory suggests that *o*-addition is dominant with branching ratio of ~95% at 298 K. Therefore, only the fate of *o*-adduct (denoted as P2 below) was considered here for simplicity. In the atmosphere, the adduct P2 will react with O₂, NO, and NO₂, for which rate constants have been measured as $\sim 2 \times 10^{-14}$, $< 0.7 \times 10^{-13}$, and $\sim 3 \times 10^{-11}$ cm³ molecule^{−1} s^{−1}, respectively.^{8,18} Under the atmospheric conditions (NO_x ~ tens of ppbv), the adducts would react with O₂ predominantly, even though nitrophenol has been observed in laboratory studies with NO_x at tens of ppm level.^{10–13} On the other hand, the rate constants are lower by orders of magnitude for reactions between O₂ and adducts of OH with other aromatic compounds such as benzene and naphthalene,^{8,18} for which the reactions of the OH adducts with NO₂ are important even at ambient concentrations in forming toxic aromatic nitrates.^{18,19}

3.2. Reaction Between Phenol–OH *ortho*-Adduct (P2) and O₂. In analogy to the reactions of the OH adducts of benzene^{20,21} and naphthalene,^{22–24} the reaction of P2 and O₂ would proceed by O₂ additions and direct H-abstraction from C₂ position (Scheme 1), of which H-abstraction leads to the formation of catechol. O₂ addition to P2 can occur at C₁, C₃, and

Scheme 1. Reaction of P2 and O₂



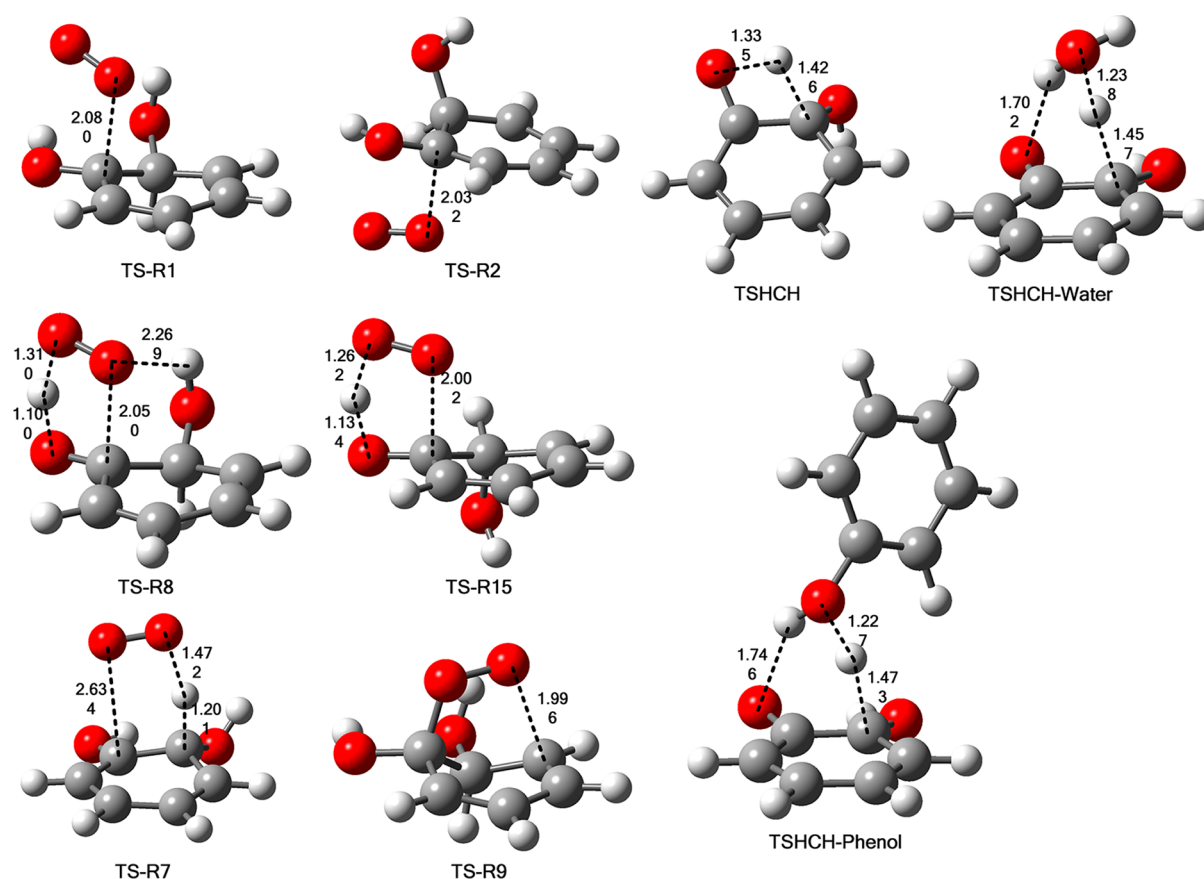


Figure 2. BH&HLYP/6-311++G(2df,2p) geometries for selected transition states in reaction of P2 radical and O₂ (bond lengths in Å).

Table 1. Calculated Reaction Energies (in kJ/mol) at Levels of BH&HLYP/6-311++G(2df,2p) (DFT) and ROCCSD(T)/6-311+G(d,p) (ROCC) and the Predicted Forward and Reverse Rate Constants (in cm³ molecule⁻¹ s⁻¹ for Bimolecular Reactions and in s⁻¹ for Unimolecular Reactions) Based on ROCCSD(T) Energies

number: reactions	DFT	ROCC		DFT	ROCC		k_{Forward}	k_{Reverse}
	$\Delta E_{0\text{K}}$	$\Delta E_{0\text{K}}$	$\Delta G_{298\text{K}}$	$\Delta E_{0\text{K}}^{\ddagger}$	$\Delta E_{0\text{K}}^{\ddagger}$	$\Delta G_{298\text{K}}^{\ddagger}$		
R ₁ : P2 + O ₂ → P2-1OO- <i>syn</i>	-17.5	-53.8	-7.8	33.2	-13.5	31.2	8.54×10^{-13}	9.07×10^5
R ₂ : P2 + O ₂ → P2-1OO- <i>anti</i>	-14.9	-48.7	-4.5	38.7	-8.5	34.3	2.49×10^{-13}	9.79×10^5
R ₃ : P2 + O ₂ → P2-3OO- <i>syn</i>	-13.3	-47.9	-4.2	50.2	15.8	56.6	3.00×10^{-17}	1.36×10^2
R ₄ : P2 + O ₂ → P2-3OO- <i>anti</i>	-16.0	-47.6	-4.1	46.2	9.6	50.5	3.57×10^{-16}	1.65×10^3
R ₅ : P2 + O ₂ → P2-5OO- <i>syn</i>	-20.8	-33.7	12.5	50.2	20.5	61.3	4.49×10^{-18}	1.72×10^4
R ₆ : P2 + O ₂ → P2-5OO- <i>anti</i>	-23.9	-36.8	8.1	56.9	10.8	53.3	1.13×10^{-16}	7.21×10^4
R ₇ : P2 + O ₂ → catechol + HO ₂ ^a	-111.3	-100.6	-102.6	45.7	8.8	51.4	8.21×10^{-16}	
R ₈ : P2-1-OO- <i>syn</i> → HCH + HO ₂ <i>syn</i>	8.4	31.3	-17.3	46.1	39.0	38.6	1.08×10^6	
R ₉ : P2-1-OO- <i>syn</i> → P2-1,3-OO- <i>syn</i>	-14.1	-18.9	-16.1	63.5	47.6	52.1	4.58×10^3	6.99×10^0
R ₁₀ : P2-1-OO- <i>syn</i> → P2-1,4-OO- <i>syn</i>	76.5	68.5	71.8	135.0	115.3	118.0	1.27×10^{-8}	4.90×10^4
R ₁₁ : P2-1-OO- <i>syn</i> → P2-1,5-OO- <i>syn</i>	64.4	57.0	60.6	152.2	133.5	136.9	6.28×10^{-12}	2.58×10^{-1}
R ₁₂ : P2-1-OO- <i>syn</i> → P2-1,6-OO- <i>syn</i>	24.8	31.8	31.9	101.7	95.3	97.5	4.97×10^{-5}	1.96×10^1
R ₁₃ : P2-1-OO- <i>syn</i> → H-Shift (C ₁ -OH)				129.0	100.4	101.1	1.20×10^{-5}	
R ₁₄ : P2-1-OO- <i>syn</i> → H-Shift (C ₂ -OH)				106.8	91.7	94.9	1.45×10^{-4}	
R ₁₅ : P2-1-OO- <i>anti</i> → HCH + HO ₂ <i>anti</i>	5.8	26.3	-20.6	54.8	42.0	42.7	2.07×10^5	
R ₁₆ : P2-1-OO- <i>anti</i> → P2-1,3-OO- <i>anti</i>	-7.2	-13.7	-8.7	94.2	76.7	81.3	3.44×10^{-2}	1.01×10^3
R ₁₇ : P2-1-OO- <i>anti</i> → P2-1,4-OO- <i>anti</i>	76.3	67.5	72.2	136.4	116.4	121.0	3.84×10^{-9}	1.73×10^4
R ₁₈ : P2-1-OO- <i>anti</i> → P2-1,5-OO- <i>anti</i>	58.8	49.1	54.4	156.8	137.4	140.3	1.59×10^{-12}	5.36×10^{-3}
R ₁₉ : P2-1-OO- <i>anti</i> → P2-1,6-OO- <i>anti</i>	27.7	28.9	32.3	108.8	102.3	104.7	2.74×10^{-6}	1.27×10^0
R ₂₀ : P2-1-OO- <i>anti</i> → H-Shift (C ₂ -H)				113.3	96.2	100.6	1.44×10^{-5}	
R ₂₁ : HCH → catechol	-102.2	-78.2	-77.5	288.0	273.0	273.4		
R ₂₂ : HCH → catechol (with H ₂ O)	-102.2	-78.2	-77.5	103.0				
R ₂₃ : HCH → catechol (with C ₆ H ₅ OH)	-102.2	-78.2	-77.5	110.0				

^aDirect hydrogen abstraction with tunneling correction factor of 3.26.

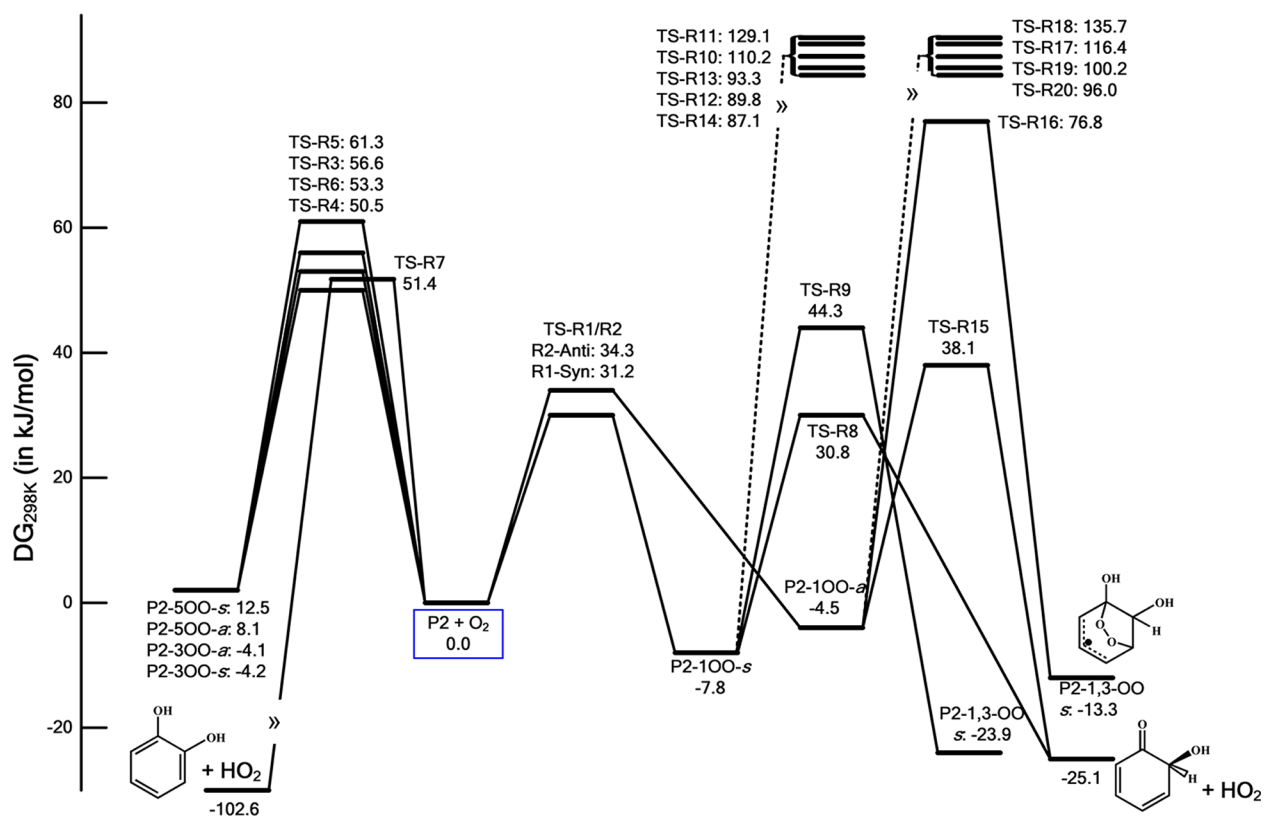


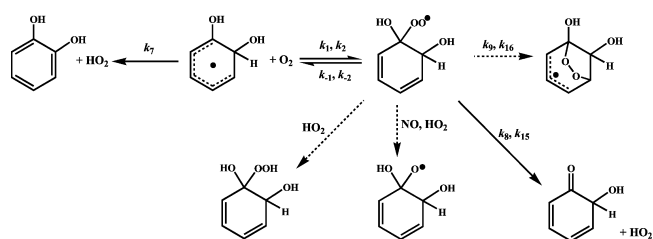
Figure 3. Gibbs energies for the reaction of P2 adduct with O_2 at ROCCSD(T)/6-311+G(d,p)//BH&HLYP/6-311++G(2df,2p) level.

C_5 positions from *syn* and *anti* directions, forming P2-*n*-OO-*a/s* ($n = 1, 3, 5$, and *a/s* = *anti/syn*). Figure 2 shows the geometries of selected transition states. Table 1 lists the reaction energetics at levels of BH&HLYP and ROCCSD(T)/6-311+G(d,p), and Figure 3 sketches the Gibbs energy changes at ROCCSD(T)/6-311+G(d,p) + ZPE//BH&HLYP level. The BH&HLYP calculations, even as DFT method, are strongly spin-contaminated for species containing one unpaired aromatic π -electron and all the transition states but not for P2-*n*-OO, e.g., $\langle S^2 \rangle$ of 0.833 and 0.758 for P2 and P2-1-OO-*syn*, and of 1.212, 1.195, and 1.220 for transition states of R_1 , R_2 , and R_7 , respectively. Consequently, the BH&HLYP reaction energies and barrier heights are greatly overestimated if compared to the ROCCSD(T) ones (Table 1). Discussions below will be based on the ROCCSD(T) energies. It is noticed that the barriers for R_1 and R_2 (O_2 additions to C_1) are below the separate $P2 + O_2$. This is again due to the possible prereactive complexes between P2 and O_2 , though such complexes are not searched here.

In analogy to the similar peroxy radicals in oxidations of benzene and naphthalene,^{20–24} P2-1-OO-*s/a* can undergo back-decomposition to $P2 + O_2$ (R_{-1} and R_{-2} in Table 1), ring-closures to bicyclic radicals P2-1,*m*-OO (R_9 – R_{12} and R_{16} – R_{19}), intramolecular H-shifts (R_{13} , R_{14} , and R_{20}), and concerted eliminations of HO_2 from P2-1-OO-*s/a* to form 2-hydroxy-3,5-cyclohexadienone (**HCH**, R_8 and R_{15} , Scheme 1). The transition states for R_8 and R_{15} were confirmed by IRC calculations (Figure S1), while the transition state for possible concerted HO_2 elimination from P2-1-OO-*a* to form catechol directly could not be identified despite extensive search. Bimolecular reactions with NO and HO_2 are also possible for P2-1-OO-*s/a* in the atmosphere or in simulation smog chambers. Among the unimolecular processes for P2-1-OO-*s*, HO_2 -elimination (R_8) and back-decomposition (R_{-1}) have the lowest barriers, while

the ring-closure to P2-1,3-OO-*s* (R_9) has a barrier 13.5 kJ/mol higher than the HO_2 elimination (Table 1, Figure 3). For P2-1-OO-*a*, the barriers for HO_2 -elimination and back-decomposition are comparable, while the barrier for ring-closure to P1-1,3-OO-*a* is higher by ~ 30 kJ/mol. Transition states for intramolecular H-shifts and other ring-closures are higher by at least 30 kJ/mol, rendering their negligible role in the atmospheric oxidation of phenol.

After simplification, the reaction scheme of P2 and O_2 could be reduced to



Assuming high pressure limit, the unimolecular rate constants could be estimated as 9.1×10^5 , 1.1×10^6 , and 4.6×10^3 s^{-1} for k_{-1} , k_8 , and k_9 of P2-1-OO-*s* and as 9.8×10^5 , 2.1×10^5 , and 3.4×10^{-2} s^{-1} for k_{-2} , k_9 , and k_{16} of P2-1,3-OO-*a* at 298 K (Table 1), using $k = (k_B T/h) \exp[-\Delta G^\ddagger/RT]$, where ΔG^\ddagger is the Gibbs barrier height.²⁵ The HO_2 eliminations (k_8 and k_{15}) are several orders of magnitude higher than ring-closures to P2-1,3-OO (k_9 and k_{16}) for both *syn* and *anti* conformers. The bimolecular reactions of P2-1-OO with NO or HO_2 are also slow, at rates of $\sim 10^0$ s^{-1} , assuming 5 ppb concentrations for NO and HO_2 and rate constants of 10^{-11} cm^3 molecule $^{-1}$ s^{-1} . Reaction of P2-1-OO with NO cannot compete with HO_2 elimination even with [NO] up to 2.4×10^{14} molecule cm^{-3} (~ 10 ppmv).² Assuming steady state for P2-1-OO, the effective bimolecular rate constants ($k_{b,eff}$)

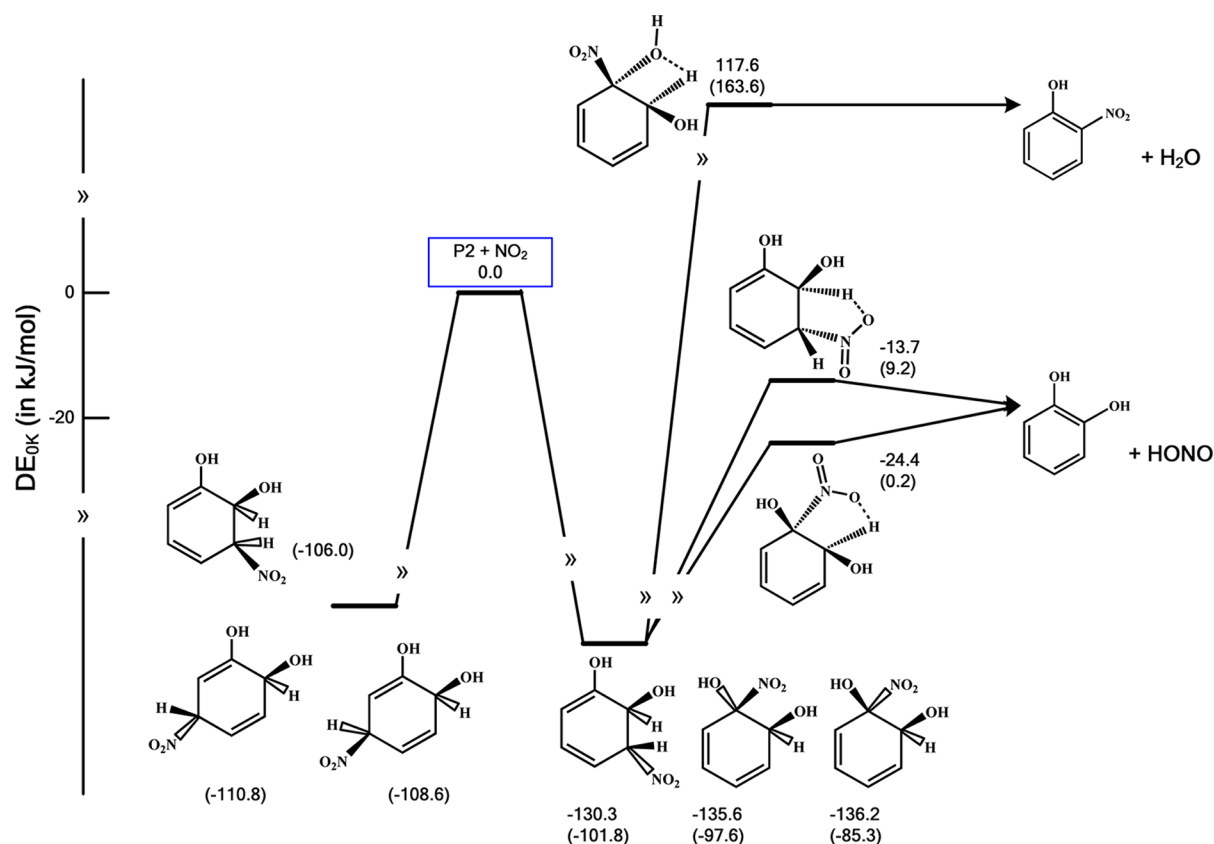


Figure 4. Relative energies for the reaction of P2 adduct with NO₂ at ROCCSD(T) and BH&HLYP (in parentheses) levels.

for P2 and O₂ through the addition route can be estimated as $\sim 5.1 \times 10^{-13} \text{ cm}^3 \text{ molecule}^{-1} \text{ s}^{-1}$ for *syn* and *anti* conformers, respectively, at 298 K by using

$$k_{b,\text{eff}} = k_1 k_8 / (k_{-1} + k_8) + k_2 k_{15} / (k_{-2} + k_{15})$$

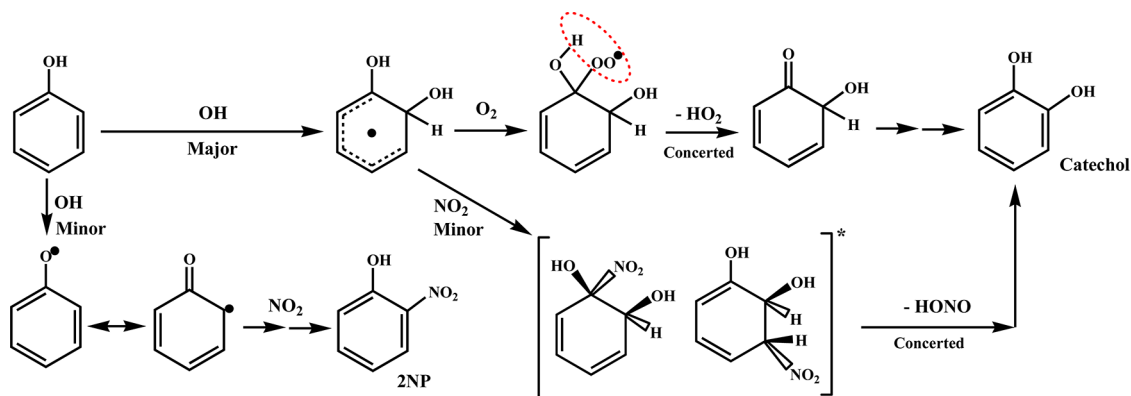
k_b for direct H-abstraction can also be estimated as $8.2 \times 10^{-16} \text{ cm}^3 \text{ molecule}^{-1} \text{ s}^{-1}$, including the tunneling correction with the asymmetric Eckart model.²⁶ The estimated overall $k_{b,\text{eff}}$ of $\sim 5.1 \times 10^{-13} \text{ cm}^3 \text{ molecule}^{-1} \text{ s}^{-1}$ is about 1 order of magnitude higher than the experimental value of $\sim 2 \times 10^{-14} \text{ cm}^3 \text{ molecule}^{-1} \text{ s}^{-1}$,^{8,18} however, the dominance of the O₂ addition pathway and therefore formation of HCH is obvious.

The dominance of O₂ addition over H-abstraction for the reaction between P2 and O₂ is different from that for the reaction between C₆H₆–OH and O₂, for which the yield of phenol from direct H-abstraction is ~ 0.5 .¹ It is noticed that for C₆H₆–OH + O₂, the barrier heights for direct H-abstraction, O₂ addition, and subsequent concerted HO₂-elimination are comparable, as 16.9, 11.1 (*syn* addition), or 16.8 (*anti* addition), and 20.7 kJ/mol, respectively, at G3XMP2-RAD level.²⁰ The corresponding values for P2 + O₂ are 8.8, –13.5, and –14.8 kJ/mol (Table 1, for P2-1OO-*syn*). Similarly for 2,7-dimethyl naphthalene, the barrier heights for direct H-abstraction and O₂ addition are 20.8 and –3.9 kJ/mol.²² Therefore, formation of catechol or naphthenol via direct H-abstraction is unlikely in oxidation of phenol or naphthalene even though formation of phenol in benzene oxidation is significant.

The formation of HCH from reaction of P2 and O₂ from current theoretical prediction is in contradiction to the experimental observations which found catechol as the main product with yields of 0.7–0.8 in phenol oxidation by OH radical

using FTIR absorption spectroscopy.^{6,14} It was noticed that HCH is much less stable than catechol by 78.2 kJ/mol at CCSD(T) level (102.2 kJ/mol by BH&HLYP); therefore catechol may be formed from HCH through a keto–enol tautomerization process, for which the transition state has been located at BH&HLYP level (TSHCH in Figure 2). The tautomerization is hindered by a barrier as high as 288 kJ/mol by BH&HLYP (0 K, 273 kJ/mol by CCSD(T), relative to HCH). However, it was noticed that the experimental determinations of catechol yields using FTIR were done either in a static chamber after UV irradiation for at least ten minutes¹⁴ or in a flow tube by pumping the reaction gas into a White cell continuously with total residence time of ~ 25 s or more.⁶ Indeed, our calculations show that the tautomerization can be assisted by the presence of water or phenol and transition states with one water or phenol molecule (TSHCH-Water and TSHCH-Phenol in Figure 2). The tautomerization barrier height is greatly reduced to ~ 103 kJ/mol by the presence of one water molecule or to ~ 110 kJ/mol by the presence of one phenol molecule. The tautomerization with one water or phenol molecule, with bimolecular rates of $\sim 10^{-30} \text{ cm}^3 \text{ molecule}^{-1} \text{ s}^{-1}$, is still far too slow to account for the formation of catechol. However, the barrier heights are expected to be even lower with the presence of more water or phenol molecules, and heterogeneous tautomerization on the wall may be fast and responsible for the exothermic conversion from HCH to catechol. A recent study reported tautomerization at an extremely low temperature of 28 K in argon matrix for β -cyclohexanedione, for which the barrier heights by DFT-B3LYP were also found to reduce from ~ 60 kcal/mol for isolated monomer to ~ 35 kcal/mol for hydrogen-bonded homodimer,²⁷ with both barrier heights being comparable to those for tautomerization of HCH.

Scheme 2. Summary of the Atmospheric Oxidation Pathways of Phenol



With the emergence of the HO_2 eliminations, the role of the bicyclic intermediates (P2-1,3-OO hereon) becomes negligible. This is drastically different from the oxidation mechanisms of benzene, toluene, and xylenes, where the bicyclic intermediates are important intermediates.^{20,28–32} For benzene, the reaction of the $\text{C}_6\text{H}_6\text{--OH}$ adduct with O_2 is very slow, at $10^{-16} \text{ cm}^3 \text{ molecule}^{-1} \text{ s}^{-1}$,^{8,18} because barriers for further ring-closures or H-shifts within $\text{C}_6\text{H}_6\text{--OH--O}_2$ are higher than its back-decomposition by at least 15.1 kJ/mol (by G3XMP2-RAD).²⁰ Similarly for naphthalene by 21.5 kJ/mol (by BB1K),²³ for 2,7-dimethyl naphthalene by 26.8 kJ/mol (by G3MP2-RAD),²² for dibenzo-*p*-dioxine by >50 kJ/mol,³³ and for other substituted benzenes. For these aromatic compounds, the reactions of the OH adducts with O_2 are expected to be slow.¹⁸ However, the concerted HO_2 eliminations create a fast drain for P2-1-OO in OH-initiated phenol oxidation, rendering the rate constants between P2 and O_2 being two or more orders of magnitude higher than other aromatics–OH adducts with O_2 .^{8,18}

3.3. Reaction Between Phenol–OH *ortho*-Adduct (P2) and NO_2 . Berndt and Boge⁶ observed the formations of catechol (~35% yield) and 2-nitrophenol (2NP, ~18% yield) with $[\text{NO}_2] \sim 1.4 \times 10^{14} \text{ molecules cm}^{-3}$ in absence of O_2 . For reaction of P2 and NO_2 , Knispel et al.⁸ obtained the rate constant of $\sim 3 \times 10^{-11} \text{ cm}^3 \text{ molecule}^{-1} \text{ s}^{-1}$. The reaction of adduct P2 and NO_2 may begin as NO_2 additions to positions 1, 3, and 5 from both *syn* and *anti* directions, forming adducts P2-*n*- NO_2 -*s/a*, of which P2-1- NO_2 -*a* and P2-3- NO_2 -*a* can lead to formation of catechol by HONO elimination and P2-1- NO_2 -*s* to 2NP by H_2O elimination. Transition states for HONO and H_2O eliminations are located at BH&HLYP level. Figure 4 shows the relative energies for the reaction of P2 adduct with NO_2 . It is found that the formations of P2- NO_2 adducts are highly exothermic ($\Delta E_{0\text{K}} \sim -130 \text{ kJ/mol}$ and $\Delta G_{298\text{K}} \sim -80 \text{ kJ/mol}$ at ROCCSD(T) level).

The transition states for HONO eliminations (forming catechol) from P2-1- NO_2 -*a* and P2-3- NO_2 -*a* are below the separated P2 and NO_2 by 24.4 and 13.7 kJ/mol, respectively, being consistent with the observed high yields of catechol from P2 and NO_2 in the absence of O_2 .⁶ Similar mechanisms were also suggested for reactions of cresols–OH and NO_2 .³⁴ However, the transition barrier for H_2O elimination from P2-1- NO_2 -*s* to form 2NP is more than 100 kJ/mol above the separate reactants P2 and NO_2 ; therefore, the experimentally observed 2NP arises unlikely from the reaction between P2 and NO_2 . The most likely source for 2NP might be the reaction of phenoxy radical with NO_2 . The detail of reaction from phenoxy radical and NO_2 to 2NP is desired.

4. CONCLUSIONS

The gas-phase oxidation mechanism of phenol initiated by OH radical was investigated at ROCCSD(T)/6-311+G(d,p)//BH&HLYP/6-311++G(2df,2p) level. The oxidation pathways are summarized in Scheme 2. The initial step for phenol and OH reaction is dominant by OH addition to *o*-position, forming P2. Under the atmospheric conditions, P2 would combine with O_2 at the *ipso*-position dominantly to form P2-1-OO adduct, which subsequently eliminates HO_2 radical through a concerted process, forming HCH; while the ring-closures are negligible. The high yields of catechol observed in previous experiments^{6,14} might arise from isomerization of HCH to catechol through heterogeneous process. P2 would also react with NO_2 through addition to form P2-*n*- NO_2 ($n = 1, 3, 5$), followed by HONO-elimination to form catechol from P2-1/3- NO_2 , being consistent with the experimental observation of catechol in the absence of O_2 ,⁶ while H_2O -elimination from P2-1/3- NO_2 to form 2NP is hindered by high barriers. The source of 2NP observed in the experiment¹⁰ arises most likely from the reaction of phenoxy radical and NO_2 . However, it should be pointed out that the reaction between P2 and NO_2 is of rather minor importance in the atmosphere.

■ ASSOCIATED CONTENT

Supporting Information

Figure showing intrinsic reaction coordinates. This material is available free of charge via the Internet at <http://pubs.acs.org>.

■ AUTHOR INFORMATION

Corresponding Author

*E-Mail: wanglm@scut.edu.cn. Tel: 0086 20 87112900.

Notes

The authors declare no competing financial interest.

■ ACKNOWLEDGMENTS

Financial support from NSF China (No. 21177041) is acknowledged.

■ REFERENCES

- (1) Volkamer, R.; Klotz, B.; Barnes, I.; Imamura, T.; Wirtz, K.; Washida, N.; Becker, K. H.; Platt, U. OH-initiated oxidation of benzene Part 1. Phenol formation under atmospheric conditions. *Phys. Chem. Chem. Phys.* **2002**, *4*, 1598–1610.
- (2) Berndt, T.; Boge, O. Formation of phenol and carbonyls from the atmospheric reaction of OH radicals with benzene. *Phys. Chem. Chem. Phys.* **2006**, *8*, 1205–1214.

- (3) Atkinson, R.; Aschmann, S. M.; Arey, J.; Carter, W. P. L. Formation of ring-retaining products from the OH radical-initiated reactions of benzene and toluene. *Int. J. Chem. Kinet.* **1989**, *21*, 801–827.
- (4) Atkinson, R.; Aschmann, S. M.; Arey, J. Formation of ring-retaining products from the OH radical-initiated reactions of *o*-, *m*-, and *p*-xylene. *Int. J. Chem. Kinet.* **1991**, *23*, 77–97.
- (5) Nakao, S.; Clark, C.; Tang, P.; Sato, K.; Cocker, D., III Secondary organic aerosol formation from phenolic compounds in the absence of NO_x. *Atmos. Chem. Phys.* **2011**, *11*, 10649–10660.
- (6) Berndt, T.; Boge, O. Gas-phase reaction of OH radicals with phenol. *Phys. Chem. Chem. Phys.* **2003**, *5*, 342–350.
- (7) Borrás, E.; Tortajada-Genaro, L. A. Secondary organic aerosol formation from the photo-oxidation of benzene. *Atmos. Environ.* **2012**, *47*, 154–163.
- (8) Knispel, R.; Koch, R.; Siese, M.; Zetzsch, C. Adduct Formation of OH Radicals with Benzene, Toluene, and Phenol and Consecutive Reactions of the Adducts with NO_x and O₂. *Ber. Bunsen. Ges. Phys. Chem.* **1990**, *94*, 1375–1379.
- (9) Bolzacchini, E.; Bruschi, M.; Hjorth, J.; Meinardi, S.; Orlandi, M.; Rindone, B.; Rosenbohm, E. Gas-phase reaction of phenol with NO₃. *Environ. Sci. Technol.* **2001**, *35*, 1791–1797.
- (10) Atkinson, R.; Aschmann, S. M.; Arey, J. Reactions of OH and NO₃ radicals with phenols, cresols, and 2-nitrophenol at 296 ± 2 K. *Environ. Sci. Technol.* **1992**, *26*, 1397–1403.
- (11) Thuner, L. P.; Bardini, P.; Rea, G. J.; Wenger, J. C. Kinetics of the gas-phase reactions of OH and NO₃ radicals with dimethylphenols. *J. Phys. Chem. A* **2004**, *108*, 11019–11025.
- (12) Coeur-Tourneur, C.; Henry, F.; Janquin, M.-A.; Brutier, L. Gas-phase reaction of hydroxyl radicals with *m*-, *o*-, and *p*-cresol. *Int. J. Chem. Kinet.* **2006**, *38*, 553–562.
- (13) Coeur-Tourneur, C.; Cassez, A.; Wenger, J. C. Rate coefficients for the gas-phase reaction of hydroxyl radicals with 2-methoxyphenol (guaiacol) and related compounds. *J. Phys. Chem. A* **2010**, *114*, 11645–11650.
- (14) Olariu, R. I.; Klotz, B.; Barnes, I.; Becker, K. H. FT-IR study of the ring-retaining products from the reaction of OH radicals with phenol, *o*-, *m*-, and *p*-cresol. *Atmos. Environ.* **2002**, *36*, 3685–3697.
- (15) Raghavan, N. V.; Steenken, S. Electrophilic reaction of the OH radical with phenol. Determination of the distribution of isomeric dihydroxycyclohexadienyl radicals. *J. Am. Chem. Soc.* **1980**, *102*, 3495–3499.
- (16) Watts, J. D.; Gauss, J.; Barlett, R. J. Coupled-cluster methods with noniterative triplet excitations for restricted open-shell Hartree-Fock and other general singlet determinant reference functions. Energies and analytical gradients. *J. Chem. Phys.* **1993**, *98*, 8718–8733.
- (17) Frisch, M. J.; Trucks, G. W.; Schlegel, H. B.; Scuseria, G. E.; Robb, M. A.; Cheeseman, J. R.; Scalmani, G.; Barone, V.; Mennucci, B.; Petersson, G. A.; et al. *Gaussian 09*, Revision A.1; Gaussian: Wallingford CT, 2009.
- (18) Koch, R.; Knispel, R.; Elend, M.; Siese, M.; Zetzsch, C. Consecutive reactions of aromatic-OH adducts with NO, NO₂ and O₂: Benzene, naphthalene, toluene, *m*- and *p*-xylene, hexamethylbenzene, phenol, *m*-cresol and aniline. *Atmos. Chem. Phys.* **2007**, *7*, 2057–2071.
- (19) Nishino, N.; Arey, J.; Atkinson, R. 2-Formylcinnamaldehyde formation yield from the OH radical-initiated reaction of naphthalene: Effect of NO₂ concentration. *Environ. Sci. Technol.* **2012**, *46*, 8198–8204.
- (20) Glowacki, D. R.; Wang, L.; Pilling, M. J. Evidence of formation of bicyclic species in the early stages of atmospheric benzene oxidation. *J. Phys. Chem. A* **2009**, *113*, 5385–5396.
- (21) Olivella, S.; Sole, A.; Bofill, J. M. Theoretical mechanistic study of the oxidative degradation of benzene in the troposphere: Reaction of benzene-HO radical adduct with O₂. *J. Chem. Theory Comput.* **2009**, *5*, 1607–1623.
- (22) Zhang, Z.; Xu, X.; Wang, L. Atmospheric Oxidation Mechanism of 2,7-Dimethyl Naphthalene is Different from That of Monocyclic Aromatic Benzenes. A Theoretical Study. *J. Phys. Chem. A* **2013**, *117*, 160–168.
- (23) Zhang, Z.; Lin, L.; Wang, L. Atmospheric oxidation mechanism of naphthalene initiated by OH radical. A theoretical study. *Phys. Chem. Chem. Phys.* **2012**, *14*, 2645–2650.
- (24) Kautzman, K. E.; Surratt, J. D.; Chan, M. N.; Chan, A. W. H.; Hersey, S. P.; Chhabra, P. S.; Dalleska, N. F.; Wennberg, P. O.; Flagan, R. C.; Seinfeld, J. H. Chemical composition of gas- and aerosol-phase products from the photooxidation of naphthalene. *J. Phys. Chem. A* **2010**, *114*, 913–934.
- (25) Holbrook, K. A.; Pilling, M. J.; Robertson, S. H.; Robinson, P. J. *Unimolecular Reactions*, 2nd ed.; Wiley: New York, 1996.
- (26) Johnson, H. S.; Heicklen, J. Tunneling corrections for unsymmetrical Eckart potential energy barriers. *J. Phys. Chem.* **1962**, *66*, 532–533.
- (27) Bandyopadhyay, B.; Pandey, P.; Banerjee, P.; Samanta, A. K.; Chakraborty, T. CH—O interaction lowers hydrogen transfer barrier to keto-enol tautomerization of β -cyclohexanedione: Combined infrared spectroscopic and electronic structure calculation study. *J. Phys. Chem. A* **2012**, *116*, 3836–3845.
- (28) Baltaretu, C. O.; Lichtman, E. I.; Hadler, A. B.; Elrod, M. J. Primary atmospheric oxidation mechanism for toluene. *J. Phys. Chem. A* **2009**, *113*, 221–230.
- (29) Birdsall, A. W.; Andreoni, J. F.; Elrod, M. J. Investigation of the role of bicyclic peroxy radicals in the oxidation mechanism of toluene. *J. Phys. Chem. A* **2010**, *114*, 10655–10663.
- (30) Elrod, M. J. Kinetics study of the aromatic bicyclic peroxy radical + NO reaction: Overall rate constant and nitrate product yield measurements. *J. Phys. Chem. A* **2011**, *115*, 8125–8130.
- (31) Fang, J.; Zhang, R. Atmospheric oxidation mechanism of *p*-xylene: A density functional theory study. *J. Phys. Chem. A* **2006**, *110*, 7728–7737.
- (32) Fang, J.; Zhang, R. Density functional theory study on OH-initiated atmospheric oxidation of *m*-xylene. *J. Phys. Chem. A* **2008**, *112*, 4314–4323.
- (33) Wang, L.; Tang, A. The oxidation mechanisms of polychlorinated dibenzo-*p*-dioxins under the atmospheric conditions. A theoretical study. *Chemosphere* **2012**, *89*, 950–956.
- (34) Jorgensen, S. Gas-phase oxidation of cresol isomers initiated by OH and NO₃ radicals in the presence of NO₂. *Int. J. Chem. Kinet.* **2012**, *44*, 165–178.